UC20-G

RADIATION COOLING AND GAIN CALCULATION
FOR C VI 182 Å LINE IN C/Se PLASMA

BY

C.H. Nam, E. Valeo, S. Suckewer, and U. Feldman

APRIL 1986

PLASMA
PHYSICS
LABORATORY

PRINCETON UNIVERSITY
PRINCETON, NEW JERSEY

NOTICE

This report was prepared as an account of work sponsored by the United States Government. Neither the United States nor the United States Department of Energy, nor any of their employees, nor any of their contractors, subcontractors, or their employees, makes any warranty, express or implied, or assumes any legal liability or responsibility for the accuracy, completeness or usefulness of any information, apparatus, product or process disclosed, or represents that its use would not infringe privately owned rights.

Printed in the United States of America

Available from:

National Technical Information Service
U.S. Department of Commerce
5285 Port Royal Road
Springfield, Virginia 22161

Price   Printed Copy $ ___*___ ; Microfiche $4.50

*Pages	NTIS Selling Price	
1-25	$7.00	For documents over 600
25-50	$8.50	pages, add $1.50 for
51-75	$10.00	each additional 25-page
76-100 .	$11.50	increment.
101-125	$13.00	
126-150	$14.50	
151-175	$16.00	
176-200	$17.50	
201-225	$19.00	
226-250	$20.50	
251-275	$22.00	
276-300	$23.50	
301-325	$25.00	
326-350	$26.50	
351-375	$28.00	
376-400	$29.50	
401-425	$31.00	
426-450	$32.50	
451-475	$34.00	
476-500	$35.50	
500-525	$37.00	
526-550	$38.50	
551-575	$40.00	
567-600	$41.50	

RADIATION COOLING AND GAIN CALCULATION

FOR C VI 182 Å LINE IN C/Se PLASMA

C.H. Nam, E. Valeo, and S. Suckewer

Princeton University

Plasma Physics Laboratory

Princeton, New Jersey 08544

U. Feldman

Naval Research Laboratory

Washington, D.C. 20375-5000

MASTER

ABSTRACT

A model is developed which is capable of describing the evolution of gain resulting from both rapid radiative and expansion cooling of a recombining, freely expanding plasma. It is demonstrated for the particular case of a carbon/selenium plasma that the cooling rate which leads to optimal gain can be achieved by adjusting the admixture of an efficiently radiating material (selenium) in the gain medium (carbon). Comparison is made to a recent observation of gain in a recent NRL/Rochester experiment with carbon/selenium plasma for the n = 3 → 2 transition in C VI occurring at 182 Å. The predicted maximum gain is ~ 10 cm^{-1}, as compared to observation of 2-3 cm^{-1}.

1. INTRODUCTION

Population inversion and significant gain at wavelengths below 200 Å have been achieved in laser-produced recombining plasmas.[1] These observations are in line with theoretical calculations, which predict optimal gain conditions when:

a.) The electron temperature decreases rapidly enough so that successive ionization states of the active ion are far from equilibrium;

b.) The density is high enough so that three-body recombination, which occurs principally into upper quantum levels, is the dominant recombination mechanism;

c.) The density is not too high, however, lest collisions quench the inversion; and

d.) Optical trapping is not important.

These conditions have been achieved experimentally in magnetically confined carbon plasma created and heated by a CO_2 laser.[1,2] (The magnetic field not only maintains the desired high density, but has the additional advantage that the confined plasma has good uniformity along the field, thereby providing a long gain path.) Inversions between principal quantum numbers $n = 3$ and $n = 2$ (182 Å) and between $n = 4$ and $n = 2$ (135 Å) of the hydrogen-like carbon ion were observed after the laser pulse. In these experiments, the required rapid cooling is principally due to line radiation from the carbon. If, however, additional cooling is required, it has been shown both experimentally[3] and theoretically[4] that the inclusion of a somewhat higher atomic number material, such as aluminum, in the target plasma composition provides an effective increase in the cooling rate.

If, however, such a plasma is allowed to freely expand in the absence of a confining field, then the radiative cooling rate decreases with the

density. Although this reduced efficiency of radiation is offset to some extent by cooling due to expansion, one expects that the inclusion in the plasma of relatively more efficient radiators, for instance materials with yet higher atomic number, is required in order to achieve gain conditions.

Evidence for the importance of radiative cooling in creating conditions for gain in a freely expanding plasma is contained in the results of a recent NRL/Rochester experiment.[5] In these experiments, a thin foil target of selenium and formvar $(C_{11}H_{18}O_5)$ was illuminated with 0.35 micron radiation from the powerful OMEGA laser. A line focus of up to 13.6 mm length was used. The 182 Å line of C VI was observed to be enhanced axially. Because of its higher atomic number, selenium provides the dominant radiative cooling.

Motivated by these physical considerations and experimental results, we have developed a computational model which enables us to investigate the combined effects of both adiabatic cooling and radiative cooling by admixtures in order to find conditions for gain in recombining hydrogen-like carbon. A significantly greater level of detail is required to accurately compute gain than to compute total radiated power. We therefore describe the evolution of the carbon ions with a set of rate equations which not only describe transitions between ionization stages, but also, for hydrogen-like carbon, between the upper levels as well. On the other hand, in computing radiative losses from a high atomic number admixture, we employ a version of the less-detailed hydrogenic average ion description,[6,7] modified to take account of the nonequilibrium collisional-radiative conditions of interest. The effects of hydrodynamic expansion are included in our otherwise homogeneous, cylindrical model by assuming a radial velocity profile of the form $v(r,t) = \{r/R(t)\}\, dR(t)/dt$ and employing energy and momentum conservation to determine $R(t)$.

The model is described in detail in Section 2. Applications are made in Section 3. First, radiative cooling of a carbon/aluminum plasma at constant volume is calculated and compared with more detailed calculations.[8] This comparison demonstrates the accuracy of the average ion model for radiative cooling calculations. Next, application is made to carbon/selenium plasma, including expansion. The dependence of the magnitude and time evolution of population inversion on radiative and expansion cooling rates is shown. Optimal conditions for gain are obtained by varying the fractional composition of carbon and selenium and the initial plasma size. Conclusions are drawn in Section 4.

2. COMPUTATIONAL MODEL

Our interest is in computing the evolution of a carbon/selenium plasma during the fast recombination phase. We idealize the NRL/Rochester experimental geometry[5] by assuming that the plasma has already expanded by an amount comparable to the width of the laser focal line (about 100 microns) and has taken on a cylindrical shape. We also assume that complete mixing of carbon and selenium has occurred during this initial expansion phase. Our calculations model the subsequent evolution of this homogeneous, cylindrical plasma.

A. Carbon

The collisional-radiative model[9] is used to compute the evolution of the ground state densities $N_1^j(t)$ of each ionization stage. The governing rate equations are

$$\frac{dN_1^j}{dt} = (N_1^{j-1} S_1^{j-1} - N_1^j S_1^j) \, N_e$$

$$+ (N_1^{j+1} \alpha_c^{j+1} - N_1^j \alpha_c^j) N_e \qquad\qquad (1)$$

for $j = 0, 1, \ldots, 6$. Here, $S_1^j(T_e)$ and $\alpha_c^j(T_e, N_e)$ are the rate coefficients for collisional ionization and for collisional-radiative recombination, respectively. Only collisional ionization from the ground state is included for calculational simplicity. For C VI ions, this approximation is quite accurate throughout the temperature range of interest. When the temperature is greater than ~ 200 eV, the density is also high ($N_e > 5 \times 10^{20}$ cm^{-3}), and all the excited states are in local thermodynamic equilibrium (LTE) with the free electrons and the fully stripped carbon ions. Under these conditions, ionization from the excited states is taken into account by the collisional-radiative model.[10,11] At lower temperatures, the recombination rate dominates the ionization rate even when the contribution from the excited states is included. The rate coefficient for collisional-radiative recombination[12] includes both three-body recombination and photorecombination, and takes into account the contributions to recombination due to cascade through highly excited states.

B. Average Ion Model

The evolution of the radiator ions is calculated by employing a screened hydrogenic average ion model.[6,7] In this model, as in the Fermi model of the atom, the electrons are treated as a fluid. The model replaces the set of ions with discrete charge states i by a single "average ion" with occupation numbers P_n equal to the average of the P_n^i for each charge state i over all charge states:

$$P_n = \sum_i f_i P_n^i \quad .$$

Here, f_i is the fraction of the ion with charge i. The energy of the nth shell, E_n, is written as

$$E_n = E_n^O - Ry \frac{Z_n^2}{n^2} \quad , \tag{2}$$

where $Ry = e^2/2a_0$ with $a_0 = \hbar^2/m\, e^2$. The first term, E_n^O, is the electrostatic potential arising from electrons outside shell n, while the second term is the potential due to the nuclear charge Z as screened by electrons with principal quantum number $n' < n$. The interaction of electrons within shell n is accounted for by assigning half of them to outer shells and half to inner shells. These effects are included through the introduction of screening constants, $\sigma(n, m)$, which describe the screening of the nth shell by the mth. Specifically,

$$E_n^O = \frac{1}{2} \frac{e^2}{r_n} \sigma(n,n)\, P_n + \sum_{m>n} \frac{e^2 P_m}{r_m} \sigma(m,n) \quad , \tag{3}$$

and

$$Z_n = Z - \sum_{m<n} \sigma(n,m)\, P_m - \frac{1}{2} \sigma(n,n)\, P_n \quad , \tag{4}$$

where $r_n = a_0 n^2/Z_n$ is the radius of shell n. The average ionization state $\bar{Z}$ is then

$$\bar{Z} = Z - \sum_n P_n \quad . \tag{5}$$

We employ More's screening constants,[7] which give a more accurate value for the ionization potential, especially for $\bar{Z} \ll Z$, than do the original values due to Mayer.[13]

The shell structure of the average ion is described by three classifications: Local Thermodynamic Equilibrium (LTE) shells, inner shells, and collisional-radiative shells. For those electrons in shells with large quantum number, collisional processes dominate radiative processes. Consequently, these electrons are in local thermodynamic equilibrium with free electrons. These LTE shells are populated according to the Fermi-Dirac distribution,

$$P_n = \frac{2n^2}{1 + \frac{2}{N_e}\left(\frac{mT_e}{2\pi\hbar^2}\right)^{3/2} \exp\left(-\frac{|E_n|}{T_e}\right)} \quad , \tag{6'}$$

which can be approximated by the Saha-Boltzmann distribution,

$$P_n = n^2 \, N_e \left(\frac{2\pi\hbar^2}{mT_e}\right)^{3/2} \exp\left(\frac{|E_n|}{T_e}\right) \quad , \tag{6}$$

because the levels are nondegenerate, i.e., $P_n \ll 1$. Equation (6) is applicable for $n_{LTE} \leq n \leq n_{max}$ where the principal quantum number n_{LTE} is chosen so as to give a smooth transition to the collisional-radiative shells, and n_{max} is the total number of shells kept in the model. We find values for n_{LTE} and n_{max} of about 10 and 15, respectively, to be adequate for our calculations.

The inner shells are those n_I filled shells for which the excitation rate is negligibly small. For any inner shell, the population is given by

$$\frac{dP_n}{dt} = 0 \text{ and } P_n = 2n^2; \ n \leq n_I \quad . \tag{7}$$

The $(n_I + 1)^{th}$ shell is the effective ground state.

The populations of the collisional-radiative shells are described by the set of rate equations,

$$\begin{aligned}
\frac{dP_n}{dt} &= \sum_{j=n+1}^{n_{max}} \left\{ (N_e S_{jn} + A_{jn}) \, P_j Q_n - N_e S_{nj} P_n Q_j \right\} \\
&+ \sum_{j=n_I+1}^{n-1} \left\{ N_e S_{jn} P_j Q_n - (N_e S_{nj} + A_{nj}) \, P_n Q_j \right\} \\
&- N_e (S_n P_n - N_e \beta_n) \quad ,
\end{aligned} \tag{8}$$

for $n = n_I + 1, \ n_I + 2, \ \ldots \ldots n_{LTE} - 1$. In Eq. (8), $S_{ij}(T_e)$ and A_{ji} $(j > i)$ are the rate coefficients for collisional excitation and for radiative decay. S_n and $\beta_n(T_e)$ are the rate coefficients for collisional ionization and for direct three-body recombination to the shell n, respectively. Hydrogenic oscillator strengths modified as given in Eqs. (A21) and (A22) of Ref. 6 are used in these rate coefficients. $Q_n = 1 - P_n/2n^2$ is the vacancy factor for the nth shell which takes into account the availability of the final state in a transition. In Eq. (8), the contributions from dielectronic recombination and from photorecombination are neglected because, for high electron density plasma, the net three-body recombination to highly excited levels dominates both of these effects.

C. Hydrodynamics

Consistent with our assumption of a uniform cylindrical plasma, we assume a radial velocity profile of the form

$$v(r,t) = \frac{r}{R(t)} u(t) \quad , \tag{9}$$

with $u(t) = dR(t)/dt$ the speed of the plasma boundary $R(t)$. Neglecting atomic processes for the moment (we include them in a full energy balance in Section 2.D), the transformation of internal energy to directed energy of expansion is described by the energy conservation equation,[14]

$$P \frac{dV}{dt} = - \frac{d}{dt} \left(\frac{1}{2} \bar{M} u^2 \right) \quad . \tag{10}$$

Here,

$$P = \frac{N_{e,T}}{V} T_e \tag{11}$$

is the pressure of the total number $N_{e,T}$ of electrons confined to the volume $V = \pi R^2 L$ of the cylindrical plasma of fixed axial length L. A small contribution to the pressure from ion thermal motion is neglected in Eq. (11). The "effective mass" $\bar{M}$ is related to the total ion mass M_T by

$$\bar{M} \equiv M_T \frac{\int d^3 x \, v^2}{u^2 V} = \frac{1}{2} M_T \quad . \tag{12}$$

Combining Eqs. (9) through (12), we obtain

$$\frac{du}{dt} = \frac{2N_{e,T}}{\bar{M}} \frac{T_e}{R} \tag{13}$$

for the acceleration of the boundary.

The rate of change of electron thermal energy (cooling) due to expansion is given by

$$\frac{3}{2} N_{e,T} \frac{dT_e}{dt} = - \frac{d}{dt} \left(\frac{1}{2} \bar{M} u^2 \right) \quad . \tag{14}$$

With the neglect of radiation, the left hand sides of Eqs. (10) and (14) may be equated and the plasma radius and electron temperature are seen to satisfy the adiabatic relation,

$$T_e R^{4/3} = \text{constant.} \tag{15}$$

D. Energy Balance

We can assemble the contributions to the evolution of the electron thermal energy $U_e(t)$:

$$\frac{dU_e(t)}{dt} \equiv \frac{3}{2} \frac{d}{dt} (N_{e,T} T_e)$$

$$= \left(\frac{dU_e}{dt} \right)_{S_e} + \left(\frac{dU_e}{dt} \right)_c + \left(\frac{dU_e}{dt} \right)_{exp} \quad . \tag{16}$$

The first two terms are the contributions from atomic processes in the selenium ions and in the carbon ions. The last term describes cooling due to expansion as given by Eq. (14). The thermal relaxation between electrons and ions is neglected because the ion thermal energy is much smaller than the electron thermal energy.

For selenium, energy exchange with electrons through collisional excitation and de-excitation, collisional ionization, and three-body recombination are included, i.e.,

$$\left(\frac{dU_e}{dt} \right) = N_{i,Se} \, N_{e,T} \sum_{n=n_I+1}^{n_{LTE}-1} \sum_{j=n+1}^{n_{max}} \left(|E_{jn}| \right) \left(S_{jn} P_j Q_n - S_{nj} P_n Q_j \right)$$

$$- |E_n| \ (S_n P_n - N_e \beta_n)\}$$

$$- N_{i,Se} \ N_{e,T} (L_Z)_{nn} \ . \tag{17}$$

Here, $N_{i,Se}$ is the selenium ion density, $E_{jn} = E_n - E_j$ are the excitation energies, and $(L_Z)_{nn}$ are the rate coefficients which yield the radiative cooling power due to $\Delta n = 0$ transitions. These $\Delta n = 0$ transitions provide an important cooling mechanism when the temperature is much lower than the energy of the resonance transition. Their contribution is calculated by adapting the results of Ref. 6, given for a plasma in coronal equilibrium. The transition energies, E_{nn}, oscillator strengths, f_{nn}, and the Graunt factors, g_{nn}, for $\Delta n = 0$ transitions of Ref. 6 enter the modified expression,

$$(L_Z)_{nn} = S_{nn} \ E_{nn} \ \frac{A_{nn}}{A_{nn} + N_e \ S_{nn} e^{E_{nn}/T_e}} \ , \tag{18}$$

where S_{nn} and A_{nn} are the rate coefficients for collisional excitation and for radiative decay, respectively.

For *carbon*, only the dominant contribution of cooling by resonance line radiation is included because the carbon contribution to the power balance is small. Specifically,

$$\left(\frac{dU_e}{dt}\right)_c = \sum_{j=0}^{6} N_i^6 \ N_e S_{res,ex}^j \ \Delta E_{res}^j \ \frac{A^j}{N_e S_{res,de}^j + A^j} \ , \tag{19}$$

where ex and de mean excitation and deexcitation, respectively.

By *solving* Eqs. (1), (2), (5)-(8), (13)-(16), and (19), the time evolutions of plasma parameters $T_e(t)$, $N_e(t)$, $N_j^j(t)$ (j=0, 1, ..., 6) for carbon, and $P_n(t)$ for selenium are obtained.

E. Gain Calculations

We apply the relation,[9]

$$k_{ji} = \left(\frac{4\ln 2}{\pi}\right)^{1/2} \frac{1}{8\pi c} \frac{\lambda_{ji}^4}{\Delta\lambda} A_{ji} \left(N_j - \frac{g_j}{g_i} N_i\right) \quad , \tag{20}$$

for the gain per unit length, k_{ji}, for radiation interacting with a transition between levels i and j. Here, N_i are the population densities and g_i the statistical weights for the respective levels. A_{ji} is the spontaneous transition rate, λ_{ji} is the wavelength of the transition (1.82×10^{-6} cm for the $3 \rightarrow 2$ transition in C VI), and $\Delta\lambda$ is the Doppler-broadened linewidth which is obtained by assuming $T_i \approx T_e$ for $T_e < 50$ eV.

The excited state populations N_j of C VI are calculated, given N_e, N_1^6, N_1^7, T_e, and T_i, by assuming that the excited levels have reached quasi-steady state. This assumption is valid because the relaxation of the excited states is fast[15] and the population densities are small compared to the ground state population densities.

The gain relation, Eq. (20), is valid for the case in which Doppler broadening dominantly determines the width at line center. An evaluation of Stark broadening[16] due to electron impact and ion quasistatic broadening indicates that the former is larger at the line center. For the case of maximum gain presented below, impact broadening was smaller than Doppler broadening by at least a factor of two. We have therefore assumed, for simplicity, a Doppler lineshape throughout in the gain computations.

Self absorption, most importantly for the C VI L_α line, can seriously affect the gain. This is due to the decrease of the "effective" decay rate out of level 2 and the corresponding increase of N_2^5 with increasing optical

depth τ. We account for this by writing $A_{21,eff} = A_{21} \, P(\tau)$, where $P(\tau) \le 1$ is the probability of photon excape.[17] An upper bound for the C VI ground state population N_1^5 for which the L_α line remains optically thin, $\tau < 1$, and, therefore, $P(\tau) = 1$, can be estimated from the expression,[17]

$$\tau_D = \frac{\pi^{1/2} e^2 \, \lambda_{21} f_{12} N_1^5 R}{m_e c \left(\frac{2T_i}{M_i}\right)^{1/2}} \quad , \tag{21}$$

valid for a Doppler lineshape. Here, the wavelength $\lambda_{21} = 3.4 \times 10^{-7}$ cm, the oscillator strength $f_{12} = 0.42$, and all quantities are in cgs units. Taking $T_i = 4 \times 10^{-11}$ ergs (25 eV) and the plasma radius $R = 1.5 \times 10^{-2}$ cm, we obtain

$$N_1^5 \le 5.0 \times 10^{1\prime} \text{ cm}^{-3} \quad . \tag{22}$$

This is a severe limit, and is much smaller than the density at which gain has been observed in the NRL/Rochester experiment.[5] One possible explanation is that the Doppler shift due to the rapid radial expansion leads to a reduction of the effective optical depth. As shown in the Appendix, this reduction is accounted for by making the replacement

$$\tau_D \rightarrow \tau = 0.6 \, \frac{\left(\frac{2T_i}{M_i}\right)^{1/2}}{u} \, \tau_D \quad . \tag{23}$$

With a typical expansion velocity, u, of 2×10^7 cm sec^{-1}, the upper bound becomes much less restrictive, so that

$$N_1^5 \le 10^{18} \text{ cm}^{-3} \quad . \tag{24}$$

Because of the large aspect ratio $L/R \gg 1$, the axial expansion velocity is negligible for times $t \lesssim L/C_s$, where C_s is the ion acoustic velocity and the linewidth appropriate for the gain calculation, Eq. (20), is that due to thermal Doppler broadening with local temperature T_i.

3. RESULTS

In order to check the accuracy of the radiative cooling rate obtained by using the average ion model, we compared results from it with results from a more detailed collisional-radiative model[8] which contains element specific rate coefficients and energy levels. The comparison was made for a carbon/aluminum plasma at fixed volume. Sample results for the evolution of the electron temperature and for the gain, k_{32}, of the C VI H_α line are shown in Fig. 1. In this case, the carbon and aluminum densities are 2×10^{18} cm^{-3} and 6×10^{17} cm^{-3}, respectively. Initially, the carbon is taken fully stripped and the aluminum helium-like. The temperature evolution is quite comparable for the two models, with the average ion model yielding a somewhat lower temperature decay and, therefore, an upper bound for $T_e(t)$. The gains, k_{32}, obtained from the two models show close time behavior and magnitude.

For the carbon/selenium plasma, a range of plasma compositions and initial radii near the values estimated for the NRL/Rochester experiment[5] were investigated in order to examine the variation of gain evolution.

When the radiative cooling rate is relatively small, population inversion is observed, but the gain is small because the plasma has already greatly expanded and the density is low at the time of inversion. The change in electron density due to recombination of carbon and selenium is negligible compared to that due to expansion. Such a case is shown in Fig. 2(a), where

the total number of ions correspond to solid target thicknesses of carbon and selenium of 500 Å and 100 Å, respectively. The variation of electron temperature with plasma radius is seen to follow closely the adiabatic relation, Eq. (15), with the result that

$$\frac{\log[T_e(t)/T_e(o)]}{\log[N_e(t)/N_e(o)]} \cong \frac{2}{3} \quad .$$

(Note that the ratio of the vertical scales for T_e and N_e in Fig. 2(a) is 2:3.) In order to obtain high gain when expansion cooling dominates, the initial plasma radius must be much smaller than that considered here. Such would be the case in a thin carbon fiber experiment.[18]

If the selenium fraction is too large, radiative cooling is too fast, with the result that the optimal temperature range of 10–40 eV is reached when the electron density is too high. Such a case is shown in Fig. 2(b), where the initial selenium thickness has been raised to 2500 Å. The gain is quite small because the population inversion is quenched due to rapid collisional mixing of levels 2 and 3, resulting in near thermal equilibrium between them.

An optimal configuration, which was found by varying the target thicknesses, is shown in Fig. 3. The equivalent solid thicknesses of carbon and selenium are 450 Å and 1000 Å, respectively. Initial values for the plasma radius, electron temperature, and electron density are 5×10^{-3} cm, 500 eV, and 1.5 $\times$ 10^{21} cm^{-3}, respectively. The population densities of the initial ionization states are determined from steady state ionization balance, which yields almost entirely fully stripped carbon and neon-like selenium. The peak gain of 10 cm^{-1} occurs for $T_e \cong 25$ eV and $N_e \cong 5 \times 10^{19}$ cm^{-3}. The rapid rise and relatively slow decay of the gain is characteristic of an expanding plasma and is attributable to the decrease of the absolute

population densities with time. The gain exceeds 1 cm^{-1} for about 1 nsec. The radiation and expansion make approximately equal contributions to the temperature drop in this case. The time evolutions of the carbon population densities are shown in Fig. 3(b). The population densities of C VI, N_1^5, and of C VII, N_1^6, are nearly equal at the time of peak gain.

Self absorption of the C VI L_α line limits the maximum achievable gain. Increasing the amount of carbon beyond the optimum of Fig. 3 results in appreciable optical trapping, with a resultant decrease in gain as shown in Fig. 4. For target thicknesses of 600 Å and 1000 Å for carbon and selenium, shown in Fig. 4(a), self absorption reduces the gain by a factor of two relative to the optically thin result, to a value of 6 cm^{-1}. Figure 4(b) shows the effect of further increasing the carbon thickness to 1000 Å. The gain is reduced by a factor of six relative to the result obtained by neglecting trapping.

Peak gains calculated for several target compositions and for initial radii of 5×10^{-3} cm and 6.5×10^{-3} cm are presented in Table I. The roles of carbon as a lasing medium and selenium as a cooling medium are clearly seen. For target thicknesses of 400 Å for carbon and 750 Å for selenium, similar to target conditions in the NRL/Rochester experiment,[5] choosing an initial radius of 6.5×10^{-3} cm gives a gain comprable to the observed value of 2-3 cm^{-1}. For this initial radius, the largest gain, 9 cm^{-1}, is obtained for target thicknesses of 800 Å for carbon and 1000 Å selenium.

4. CONCLUSION

We have developed a model which allows a calculation of the evolution of gain in a freely expanding plasma cooled both by radiation from high atomic number components and by expansion. A comparison of the relatively simple

average ion model used to calculate radiative cooling with a more detailed code has been made for the case of carbon/aluminum plasma, which shows the accuracy of the former for this purpose. Since the average ion model allows easy replacement of radiator ion species, it is a powerful tool for the design of the target used in a recombination X-ray laser.

Application of the model to a freely expanding carbon/selenium plasma yields optimized gains approaching 10 cm^{-1}. Higher gains are unachievable due to optical trapping of the L_α line of C VI, and due to collisional mixing of levels 2 and 3 of C VI. The former mainly restricts the amount of the lasing medium (carbon) and the latter the amount of the cooling medium (selenium). With a choice of an efficient cooling element (in the sense of radiative cooling power per electron produced by the cooling medium), we may create a more favorable condition for a high gain, i.e., N_1^5 below the optical trapping limit and $N_1^6/N_1^5 \gg 1$ when T_e ($\approx T_i$) falls below 40 eV.

Acknowledgments

Table I

Peak gains in cm^{-1} obtained from different target thicknesses of carbon and selenium and initial radii. The value inside the parentheses is the gain when the optical trapping is neglected.

C/Se (Å)	R = 50 (μm)	R = 65 (μm)
400/750	6.9	2.8
300/1000	7.0	3.4
450/1000	10.3	5.2
600/1000	6.3 (13.3)	6.9
800/1000	3.9 (16.3)	9.3
1000/1000	3.1 (18.4)	4.3 (11.9)
500/1500	4.5 (10.1)	8.0 (9.0)
1000/1500	2.6 (11.4)	2.4 (15.2)
500/2000	2.8 (4.0)	4.1 (8.4)

References

1. S. Suckewer, C.H. Skinner, H. Milchberg, C. Keane, and D. Voorhees, Phys. Rev. Lett. 55, 1753 (1985).

2. S. Suckewer, C.H. Skinner, D. Voorhees, H. Milchberg, C. Keane, and A. Semet, IEEE J. Quantum Electron. QE-19, 1865 (1983).

3. H. Milchberg, C.H. Skinner, S. Suckewer, and D. Voorhees, Appl. Phys. Lett. 47, 1151 (1985).

4. C. Keane and C.H. Skinner, "Radiative Power and Electron Cooling Rates for Oxygen in Steady-States and Transient Plasma at Densities Beyond Coronal Limits," PPPL-2269 (Princeton Plasma Physics Laboratory, Princeton, NJ, 1985).

5. J.F. Seely, C.M. Brown, U. Feldman, M. Richardson, B. Yaakobi, and W.E. Behring, Opt. Commun. 54, 289 (1985).

6. D.E. Post, et al., Atomic Data and Nuclear Data Tables 20, 398 (1977).

7. R.M. More, J. Quant. Spectrosc. Radiat. Transfer 27, 345 (1982).

8. C. Keane, "Studies of XUV Population Inversion in CO_2 Laser Produced Plasmas," Ph.D. Thesis, Princeton University, 1986.

9. S. Suckewer and H. Fishman, J. Appl. Phys. 51, 1922 (1980).

10. R.W.P. McWhirter, Plasma Diagnostic Techniques, ed. by R.H. Huddlestone and S.L. Leonard, (Academic Press, New York, 1965), p. 222.

11. S. Byron, R.C. Stabler, and P.I. Bortz, Phys. Rev. Lett. 8, 376 (1962).

12. H.P. Summers, Mon. Not. R. Astron. Soc. 169, 663 (1974); "Tables and Graphs of Collisional Dielectronic Recombination Coefficients," IM367 (Appleton Laboratory, Abingdon, Oxon., 1974).

13. H. Mayer, "Methods of Opacity Calculation," LA-647 (Los Alamos Scientific Laboratory, Los Alamos, NM, 1947).

14. J.M. Dawson, Phys. Fluids 7, 981 (1964).

15. W.L. Bohn, Appl. Phys. Lett. 24, 15 (1974).

16. F.E. Irons, J. Phys. B 6, 1562 (1973).

17. T. Holstein, Phys. Rev. 72, 1212 (1947).

18. G.J. Pert, J. Phys. B 9, 3301 (1976).

Figure Captions

Fig. 1   Comparison of the average ion code with a detailed code for C/Al plasma ($n_{i,c} = 2.0 \times 10^{18}$ cm^{-3} and $n_{i,Al} = 6.0 \times 10^{17}$ cm^{-3}). The former agrees well in the Te, Ne (not shown), and gain profiles with the latter which uses specific information of Al.

Fig. 2   Two extreme cooling cases: (a) too slow cooling (C/Se = 500/100 Å) and (b) too fast cooling (C/Se = 500/2500 Å). In case (a), the plasma has already well expanded at the time of population inversion, while in case (b), population densities between levels 2 and 3 of C VI are almost thermalized because Ne is too high at Te = 10 ~ 40 eV. The arrow on the time scale shows the time of the largest gain, K_{32}, 0.2 cm^{-1} in (a) and 0.4 cm^{-1} in (b).

Fig. 3   Optimized gain case (C/Se = 450/1000 Å); (a) profiles of Te, Ne, and K_{32}, and (b) profiles of N_1^j (j = 6,5,4) and N_k^{Z-1}/g_k (k = 2,3). When the cooling rate is optimized and optical trapping is not important, the gain of the C VI 182 Å line reaches around 10 cm^{-1} from the initially fully stripped carbon and neon-like selenium.

Fig. 4   Effect of optical trapping: (a) C/Se = 600/1000 Å and (b) C/Se = 1000/1000 Å. The increase of the carbon amount from Fig. 3 cannot generate a higher gain because of the self-absorption of the C VI L_α line.

Appendix

The optical depth derived by Holstein[17] gives the value for the stationary plasma where the frequency of emitted radiation is constant in space. For the case of expanding plasma, the emitted radiation seen by an ion at a different position is Doppler-shifted by an amount which is position-dependent.

The absorption coefficient at frequency ν, $k(\nu)$, of Doppler-broadened line is given by[17]

$$k(\nu) = k_o \exp\left[-\left(\frac{\nu - \nu_o}{\nu_o}\right)^2 \left(\frac{c}{v_o}\right)^2\right] \quad , \tag{A1}$$

where ν_o is the absorption frequency at the line center of an absorbing ion,

$$k_o = \frac{\pi^{1/2} e^2 \lambda f N}{m c v_o} \quad ,$$

and $v_o = \left(\frac{2T_i}{m_i}\right)^{1/2} .$

The radiation emitted from the central region of plasma ($v(o) = 0$) is seen by an ion at r to be Doppler-shifted as

$$\nu \rightarrow \nu' = \nu \left(1 - \frac{v(r)}{c}\right)$$

$$= \nu \left(1 - \frac{u}{c}\frac{r}{R}\right) \quad ,$$

where $v(r) = (r/R)u$ is the expanding velocity at r and $u = v(R)$. So

$$\frac{\nu' - \nu_o}{\nu_o} = \frac{\nu - \nu_o - \alpha r}{\nu_o}$$

where $\alpha = (u/c)\ (\nu/R)$ is used.

The change of radiation intensity emicted at the center of plasma is given by the equation,

$$\frac{dI_\nu}{dr} = -k(\nu)\ I_\nu \ . \tag{A2}$$

By integrating Eq. (A2), we obtain

$$\frac{I_\nu(r)}{I_\nu(o)} = \exp \left[-k_o \int_o^r dr\ \exp\{ - (\frac{\nu - \nu_o - \alpha r}{\nu_o}\ \frac{c}{v_o})^2 \} \right] \ . \tag{A3}$$

Therefore, the probability of traversing a distance, r, including all the profile of Doppler-broadened emission spectrum at the center of plasma, is

$$T(r) = \int_{-\infty}^\infty \rho_D(\nu)\ \frac{I_\nu}{I_\nu(o)}\ d\nu \quad ,$$

where the Doppler-broadened line shape, ρ_D, is given by

$$\rho_D(\nu) = \frac{1}{\pi^{1/2}}\ \frac{c}{\nu_o v_o}\ \exp \left[- (\frac{\nu - \nu_o}{\nu_o}\ \frac{c}{v_o})^2 \right] \ . \tag{A4}$$

Then

$$T(r) = \frac{1}{\pi^{1/2}} \int_{-\infty}^\infty dx\ \exp\ (-x^2)\ \exp\left[-k_o \int_o^r dr\ \exp\ \{ -(x -(1 + \frac{v_o}{c}\ x)\ \frac{u}{v_o}\ \frac{r}{R}\ )^2 \} \right]$$

$$= \frac{1}{\pi^{1/2}} \int_{-\infty}^{\infty} dx \, \exp(-x^2) \, \exp\left[-k_o \exp(-x^2)\right.$$

$$\left. \times \int_{o}^{r} dr \, \exp\left\{+2x \left(1 + \frac{v_o}{c} x\right) \frac{u}{v_o} \frac{r}{R} - \left(1 + \frac{v_o}{c} x\right)^2 \left(\frac{u}{v_o} \frac{r}{R}\right)^2\right\}\right] \quad , \quad (A5)$$

where $x = \left\{(\nu - \nu_o)/\nu_o\right\} (c/v_o)$ and $(\alpha c/v_o v_o) = (\nu/\nu_o)(u/v_o)(1/R) = (1 + x \, v_o/c)$ $\times (u/v_o)(1/R)$ are used.

For the estimation of the last integral which contains the effect of the Doppler shift, consider the radiation emitted near the line center with the effective absorption radius, $\bar{r}$, such that

$$\frac{u}{v_o} \frac{r}{R} = \frac{v(r)}{v_o} \gg x \quad ,$$

$$1 + \frac{v_o}{c} x \approx 1 \quad ,$$

and $v(\bar{r}) = v_o$.

Then Eq. (A5) becomes

$$T(\bar{r}) = \frac{1}{\pi^{1/2}} \int_{-\infty}^{\infty} dx \, \exp(-x^2) \, \exp\left[-k_o \exp(-x^2) \int_o^{\bar{r}} dr \, \exp\left\{-\left(\frac{u}{v_o} \frac{r}{R}\right)\right\}\right]$$

$$= \frac{1}{\pi^{1/2}} \int_{-\infty}^{\infty} dx \, \exp(-x^2) \, \exp\left[-\frac{k_o v_o R}{u} e^{-x^2} \int_o^1 dy \, \exp(-y^2)\right]$$

$$= \frac{1}{\pi^{1/2}} \int_{-\infty}^{\infty} dx \, \exp(-x^2) \, \exp\left[-0.6 \frac{k_o v_o R}{u} \exp(-x^2)\right] \quad . \quad (A6)$$

In comparison with Eq. (2.19) of Ref. 17, the Doppler shift due to radial expansion modifies the optical depth, τ_D, of Doppler-broadened radiation as

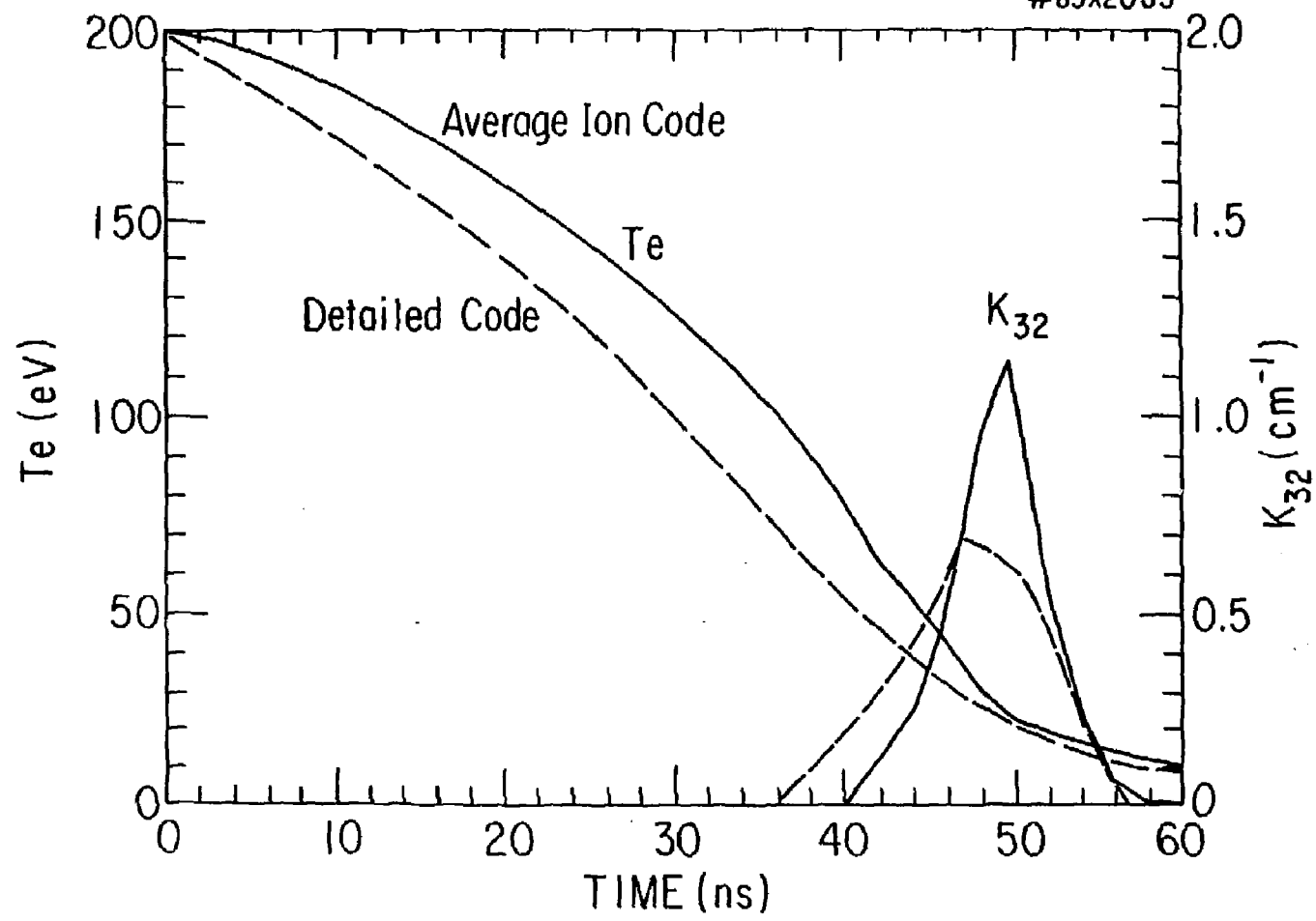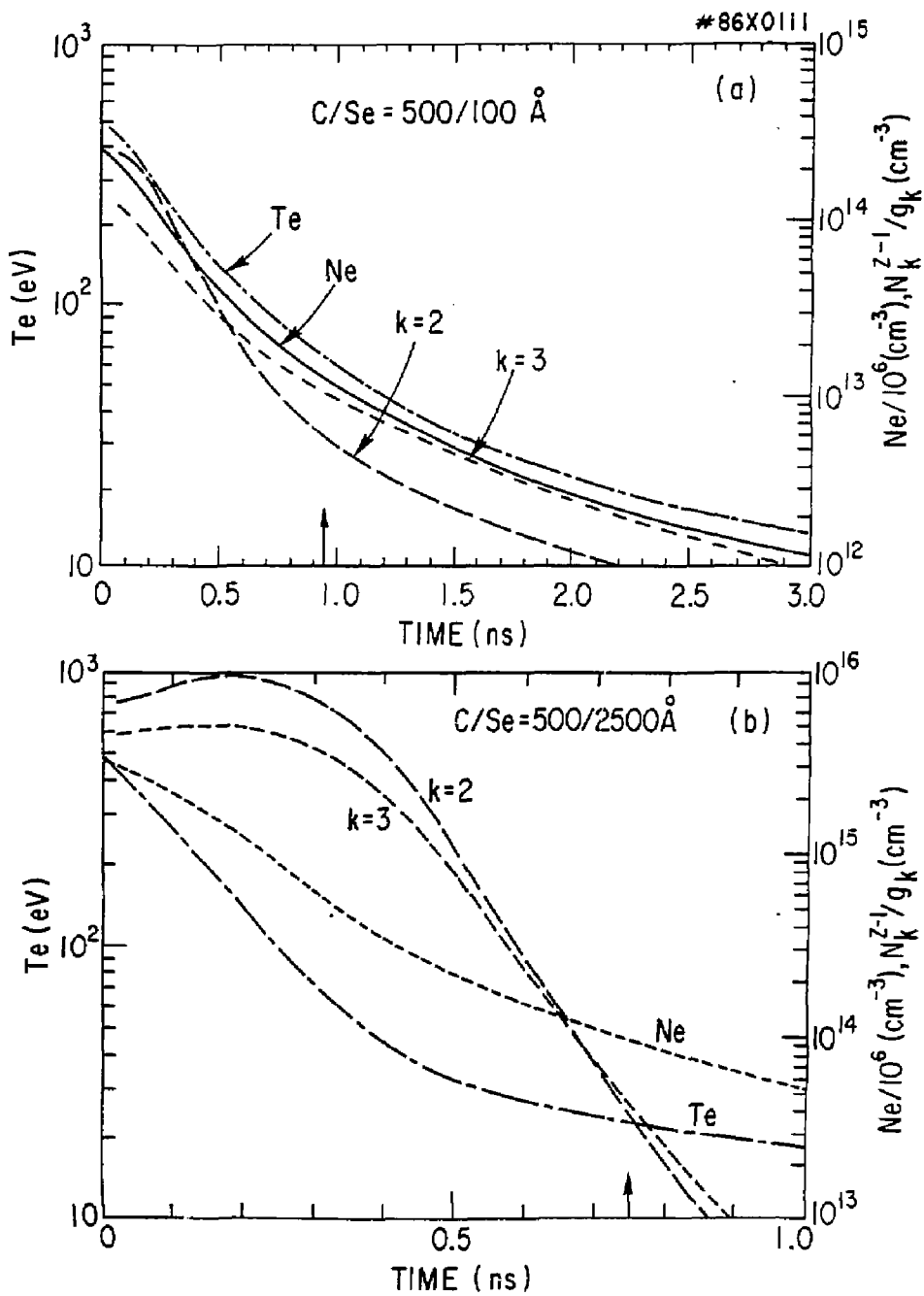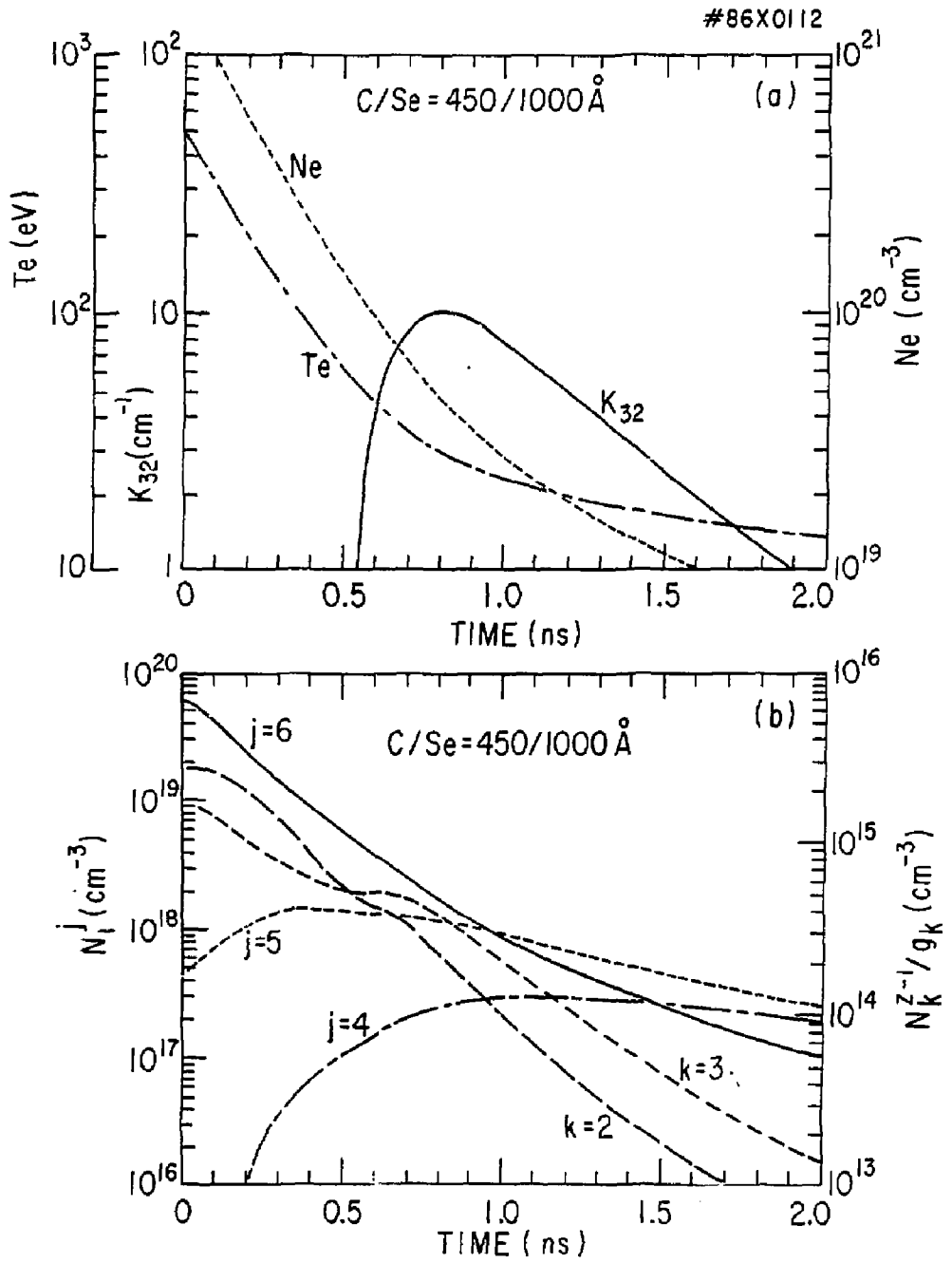$$\tau_D = k_o R + \tau = 0.6 \frac{v_o}{u} \tau_D \quad . \tag{A7}$$

Fig. 1

#86X0111

(a) C/Se = 500/100 Å

(b) C/Se = 500/2500Å

Fig. 2

#86X0112

Fig. 3

#86X0113

(a) C/Se = 600/1000 Å

(b) C/Se = 1000/1000 Å
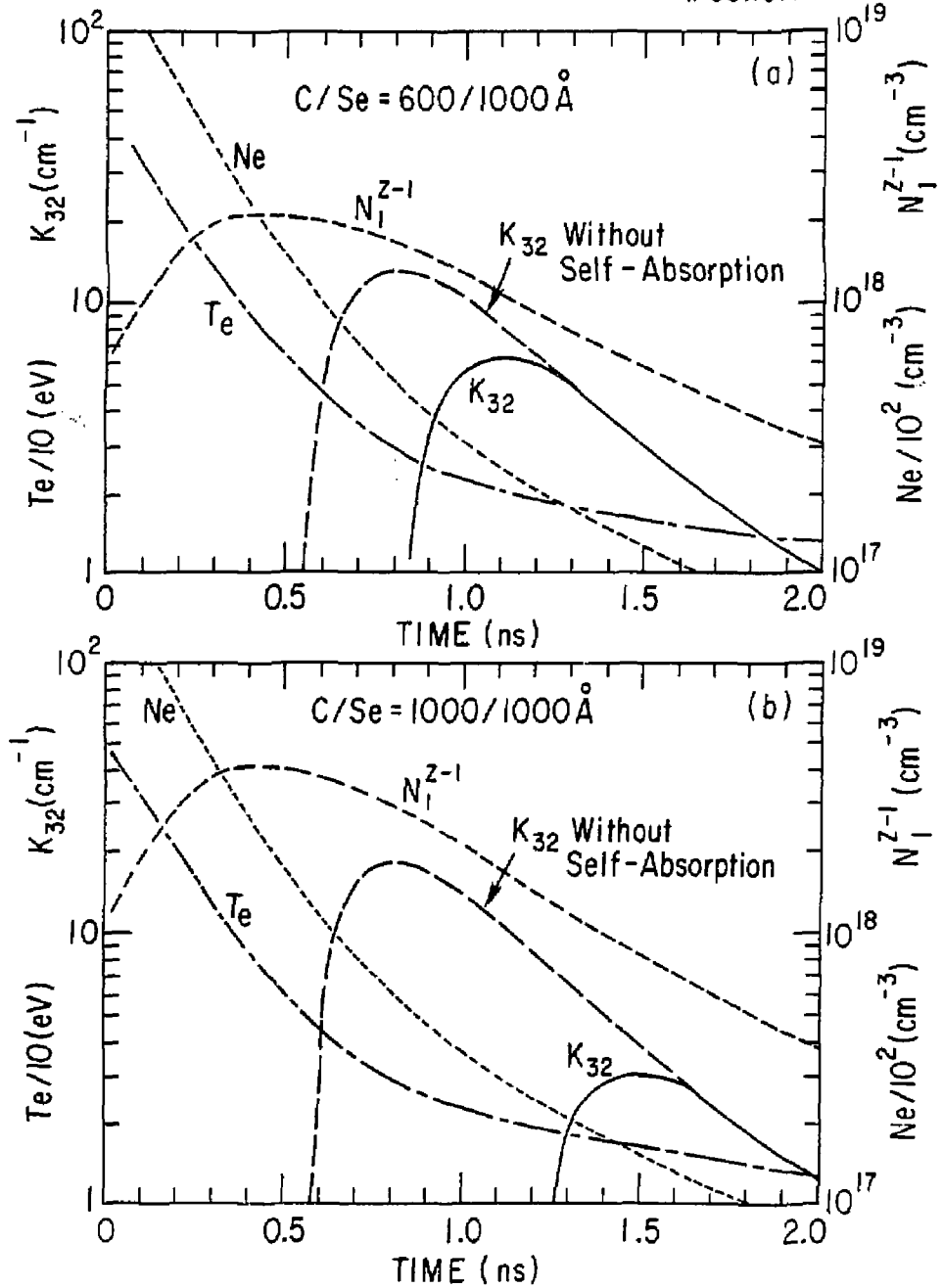
Fig. 4

Plasma Res Lab, Austra Nat'l Univ, AUSTRALIA
Dr. Frank J. Paoloni, Univ of Wollongong, AUSTRALIA
Prof. I.R. Jones, Flinders Univ., AUSTRALIA
Prof. M.H. Brennan, Univ Sydney, AUSTRALIA
Prof. F. Cap, Inst Theo Phys, AUSTRIA
Prof. Frank Verheest, Inst theoretische, BELGIUM
Dr. D. Palumbo, Dg XII Fusion Prog, BELGIUM
Ecole Royale Militaire, Lab de Phys Plasmas, BELGIUM
Dr. P.H. Sakanaka, Univ Estadual, BRAZIL
Dr. C.R. James, Univ of Alberta, CANADA
Prof. J. Teichmann, Univ of Montreal, CANADA
Dr. H.M. Skarsgard, Univ of Saskatchewan, CANADA
Prof. S.R. Sreenivasan, University of Calgary, CANADA
Prof. Tudor W. Johnston, INRS-Energie, CANADA
Dr. Hannes Barnard, Univ British Columbia, CANADA
Dr. M.P. Bachynski, MPB Technologies, Inc., CANADA
Chalk River, Nucl Lab, CANADA
Zhengwu Li, SW Inst Physics, CHINA
Library, Tsing Hua University, CHINA
Librarian, Institute of Physics, CHINA
Inst Plasma Phys, Academia Sinica, CHINA
Dr. Peter Lukac, Komenskeho Univ, CZECHOSLOVAKIA
The Librarian, Culham Laboratory, ENGLAND
Prof. Schatzman, Observatoire de Nice, FRANCE
J. Radet, CEN-BP6, FRANCE
AM Dupas Library, AM Dupas Library, FRANCE
Dr. Tom Mual, Academy Bibliographic, HONG KONG
Preprint Library, Cent Res Inst Phys, HUNGARY
Dr. R.K. Chhajlani, Vikram Univ. INDIA
Dr. B. Dasgupta, Saha Inst, INDIA
Dr. P. Kaw, Physical Research Lab, INDIA
Dr. Phillip Rosenau, Israel Inst Tech, ISRAEL
Prof. S. Cuperman, Tel Aviv University, ISRAEL
Prof. G. Rostagni, Univ Di Padova, ITALY
Librarian, Int'l Ctr Theo Phys, ITALY
Miss Clelia De Palo, Assoc EURATOM-ENEA, ITALY
Biblioteca, del CNR EURATOM, ITALY
Dr. H. Yamato, Toshiba Res & Dev, JAPAN
Direc. Dept. Lg. Tokamak Dev. JAERI, JAPAN
Prof. Nobuyuki Inoue, University of Tokyo, JAPAN
Research Info Center, Nagoya University, JAPAN
Prof. Kyoji Nishikawa, Univ of Hiroshima, JAPAN
Prof. Sigeru Mori, JAERI, JAPAN
Prof. S. Tanaka, Kyoto University, JAPAN
Library, Kyoto University, JAPAN
Prof. Ichiro Kawakami, Nihon Univ, JAPAN
Prof. Satoshi Itoh, Kyushu University, JAPAN
Dr. D.I. Choi, Adv. Inst Sci & Tech, KOREA
Tech Info Division, KAERI, KOREA
Bibliotheek, Fom-Inst Voor Plasma, NETHERLANDS
Prof. B.S. Liley, University of Waikato, NEW ZEALAND
Prof. J.A.C. Cabral, Inst Superior Tecn, PORTUGAL

Dr. Octavian Petrus, ALI CUZA University, ROMANIA
Prof. M.A. Hellberg, University of Natal, SO AFRICA
Dr. Johan de Villiers, Plasma Physics, Nucor, SO AFRICA
Fusion Div. Library, JEN, SPAIN
Prof. Hans Wilhelmson, Chalmers Univ Tech, SWEDEN
Dr. Lennart Stenflo, University of UMEA, SWEDEN
Library, Royal Inst Tech, SWEDEN
Centre de Recherchesen, Ecole Polytech Fed, SWITZERLAND
Dr. V.T. Tolok, Kharkov Phys Tech Ins, USSR
Dr. D.D. Ryutov, Siberian Acad Sci, USSR
Dr. G.A. Eliseev, Kurchatov Institute, USSR
Dr. V.A. Glukhikh, Inst Electro-Physical, USSR
Institute Gen. Physics, USSR
Prof. T.J.M. Boyd, Univ College N Wales, WALES
Dr. K. Schindler, Ruhr Universitat, W. GERMANY
Nuclear Res Estab, Julich Ltd, W. GERMANY
Librarian, Max-Planck Institut, W. GERMANY
Bibliothek, Inst Plasmaforschung, W. GERMANY
Prof. R.K. Janev, Inst Phys, YUGOSLAVIA